Journal of Civil Structural Health Monitoring (2021) 11:1239–1252
https://doi.org/10.1007/s13349-021-00507-7

ORIGINAL PAPER

Ayvalıkemer (Sillyon) historical masonry arch bridge: a multidisciplinary approach for structural assessment using point cloud data obtained by terrestrial laser scanning (TLS)

Oguzhan Safak Batar[1] · **Emre Tercan**[2] · **Engin Emsen**[1]

Received: 30 December 2020 / Revised: 17 June 2021 / Accepted: 2 July 2021 / Published online: 21 July 2021

Abstract
Historical structures are cultural heritage constituents that convey the traces and characteristic features of civilizations to the present days. One of these structures, which are among the monumental artefacts, are historical bridges. To protect historical buildings, 3D photogrammetric documentation of these structures, detailed determination of geometric and material properties and performing computer-aided structural analysis using appropriate modelling techniques are very important. The aim of this study is to present an effective, reliable, and fast multidisciplinary approach for the analysis of historical masonry bridges. The aforementioned approach is presented as an example for the behavior of the recently restored historical Ayvalıkemer (Sillyon) masonry arch bridge under possible loadings. Terrestrial laser scanning (TLS) was used to determine the bridge geometry with high accuracy. The point cloud data obtained from TLS was simplified and a three-dimensional CAD based solid model of the structure was created. This solid body has been formed the basis of the macro model for structural analysis. CDP material model was used to describe the inelastic behavior of homogenized structure. Thus, an analysis was carried out which presents the structural behavior of a historical bridge with high accuracy and reliability.

Keywords Terrestrial laser scanning (TLS) · Structural analysis · Macro modelling · Sillyon (Ayvalıkemer) · Historical structures · Masonry arch bridges

1 Introduction

Historical structures are cultural heritage constituents that convey the traces and characteristic features of civilizations to the present days [1, 2]. One of these structures, which are among the monumental artefacts, are historical bridges. Although the main purpose of bridge construction is to provide transportation, they are generally designed as piece of art. Many of these bridges vary depending on a number of factors such as material usage, design, architectural texture, inscriptions, traditional preferences [3–5]. Historical bridges built with stone materials and bearing the traces of their civilization are extremely important [6, 7]. Such architectural structures, which cannot be transported, should be preserved in the same location in the form of an open-air museum.

Masonry arch bridges are one of the most important historical bridge types. The arch form has facilitated the passage of wide openings and is therefore the most preferred form. In today's societies, cultural and socio-economic differences add originality and aesthetics to arch bridges [8–10]. However, due to its geometrical design, it is exposed to pressure. The basic building material is generally stone. Over time, deformations have been observed in bridge elements and arch forms depending on many parameters [11–13]. Historical bridges were damaged due to various effects in light and heavy direction depending on the progress of time. A number of parameters need to be known when determining the cause of the damage. These parameters include the history of the building, cracks, the type of materials used and the mechanical and chemical properties of these materials, their strength against lateral and vertical

✉ Engin Emsen
eemsen@akdeniz.edu.tr

[1] Department of Civil Engineering, Faculty of Engineering, Akdeniz University, 07058 Antalya, Turkey

[2] Department of Survey, Project and Environment, General Directorate of Highways, 13th Region, 07090 Antalya, Turkey

loads, the structure of the floor on which they are built, and error of construction [14].

To protect historical buildings, 3D photogrammetric documentation of these structures, detailed determination of geometric and material properties and performing computer-aided structural analysis using appropriate modelling techniques are very important. Calculations for determining behavior provide the basic information needed to select restoration, repair and strengthening techniques suitable for historical buildings. The existing methods used to perform the analyzes have several advantages and disadvantages depending on the approaches and assumptions used [15–17]. In historical buildings, it is necessary to interpret the behavior occurring accurately and precisely. Therefore, it is necessary to know the contents of the materials that make up the structure and the resistance of these materials under certain loads. These bridges usually consist of foundation, side wall, arch and back filling material. The materials forming the masonry structures are generally natural stone and brick. Both materials are brittle. Just like concrete, they exhibit behavior against pressure. Since mortar and masonry structures do not contain reinforcement in their components, they cannot show ductile behavior like reinforced concrete elements. Just like in reinforced concrete structures, vertical loads affect the floors to the arches, from there to the vertical bearing masonry walls and finally to the foundation. Only the moment of inertia due to lateral loads has a strong effect on masonry structures. The horizontal moment of inertia affects these loads, which exhibit rigid behavior despite the impact, on the walls with vertical bearing. However, these loads act on vertical carriers as shear and bending [18]. In masonry structures exposed to the effect of lateral loads, cracks occur in critical areas such as vertical bearing and floor joints, and this process puts the structure in the process of collapse.

There are many well-detailed studies in the literature on the structural behavior of masonry bridges. Some of these studies can be summarized as follows. Fanning and Boothby [19] used the test results of existing masonry arch bridges to determine appropriate material properties. After that, solid finite elements were used for 3D numerical analysis of bridges. The 18-span Tanaro Bridge in Italy, built in 1866 studied by Brencich and Sabia [20]. The dynamic properties of the bridge have been determined. Sevim et al. [21] conducted a study with operational modal analysis on linear seismic analysis of two historic masonry arch bridges. The 3D static non-linear behavior of masonry arch bridges analyzed by Milani and Lourenço [22]. Castellazzi et al. [23] experimentally examined the train bridge consisting of 15 openings and developed the finite element model. They decided that the bridge could be strengthened for the purpose of structural improvement. Numerous articles have been published on laser scanning measurement and three-dimensional (3D) modelling methods. Most of these articles are about the protection of cultural heritage and include different purpose structures such as historical buildings and archaeological sites and museums [24]. Dynamic evaluation of an existing three-span masonry arch bridge was studied by Pelà et al. [25]. The seismic capacity of the masonry bridge was determined by pushover and time history analyzes. Korkmaz et al. [26] have presented an analysis of the Timisvat stone arch bridge in Turkey's Rize under different lateral loads. The behavior of arch and stone bridges under different static loads evaluated by Rafiee and Vinches [27]. Altunışık et al. [28] investigated the effect of arch thickness variable on structural behavior. Stavroulaki et al. [13] are studied to prepare a realistic geometric model for 3D structural analysis of a stone arch bridge using Ground Penetrating Radar (GPR) and terrestrial photogrammetry. A hybrid method with macro and micro combination is used in the model. The effects of uncertainty in material parameters on the stochastic response in a historical masonry bridge exposed to random ground motion investigated by Hacıefendioğlu et al. [6]. The analyzes were carried out on the finite element mesh prepared by the macro modelling method of the historical masonry bridge system. Karaton et al. [29] investigated the non-linear seismic specifications of the historic twelfth century Malabadi bridge for different earthquake loads. Three different seismic load levels were selected for earthquake loading. The historical Dilovası Sultan Süleyman Bridge in Kocaeli was studied by Çakır [30]. To determine the structural behavior of the bridge, modal and response spectrum analyzes were determined using the finite element method. Drygala et al. [31] performed a seismic response analysis of a historic masonry arch viaduct located in Krakow, Southern Poland. The viaduct was modelled with ABAQUS [32] structural software program using 3D finite element model (FEM). Incremental dynamic analysis of two old railway bridges between Tehran and Kum was performed by Jahangiri al. [33] using several earthquake ground motion records. Bautista-De Castro et al. [34] proposed a multidisciplinary approach to study the reinforced concrete Bôco Bridge in Portugal, combining terrestrial laser scanner, ambient vibration testing and minor destructive testing. Caddemi et al. [35] proposed an original Discrete Macro Element Method (DMEM) that simulates masonry structures and masonry bridges with a lower computational load compared to conventional nonlinear FEM analyzes. Di Sarno et al. [36] focused on the structural performance of existing masonry and reinforced concrete bridges investigated following the 2016 Central Italian earthquakes. Analyzes have been made on bridge models to understand the true transverse failure mechanism. A macro model consisting of 3D finite elements was improved using TNO DIANA structural software. A multidisciplinary approach to determining the earthquake resistance of historical colossal

defense structures presented by Dall'Asta et al. [37]. For this purpose, geometric analysis using modern tools such as laser scanning and related point cloud processing has been used to describe the exterior and interior geometry of the large structure and to verify existing historical information. Hokelekli and Yılmaz [38] studied the in-plane and non-linear structural responses of the sidewalls of a historical masonry bridge. To this end, in 1787 the structure was built in Bartin said Turkey's history is selected masonry arch bridges. 3D finite element model and nonlinear seismic analysis of the bridge were made with ABAQUS structural software. Zhao et al. [39] proposed a two-step numerical modelling method to accomplish the difficulty in defining masonry material anisotropy and to analyze the bearing capacity of masonry arch bridges. In this modelling strategy, the masonry is selected to be a two-stage material consist of stone blocks and mortar joints. Kujawa et al. [40] prepared a study on modeling a historic church using FEM, whose geometry is based on laser scans. The aim of the study is to investigate the crushing and cracking reasons of masonry fragments. For this purpose, the FEM model of the building was prepared in ABAQUS. The homogenization procedure was applied to provide the material parameters used in the modelling. In recent years, many studies have been carried out on imaging, material characterization, modeling and seismic performance of historical bridges [41–47]. By the technological innovations, many kinds of structures could be digitally measured easily and with high accuracy. And also, many effective structural analysis programs have been developed. Therefore, it is seen that increased interdisciplinary studies that deal with these two features together and that could be benefit various engineering applications and the assessment of historical heritage [48–50].

The aim of this study is to present an effective, reliable, and fast multidisciplinary approach for the analysis of historical masonry bridges. The aforementioned approach is presented as an example for the behavior of the recently restored historical Ayvalıkemer (Sillyon) masonry arch bridge under possible loadings. Terrestrial laser scanning (TLS) was used to determine the bridge geometry with high accuracy. The point cloud data obtained from TLS was simplified and a three-dimensional CAD based solid model of the structure was created. This solid body has been formed the basis of the macro model for structural analysis. The macro modelling technique is an analysis method that well represents the behavior of large-scale masonry structures. According to this technique, masonry unit and mortar are modeled as a whole. Macro modelling technique is widely used in modelling structures such as towers, mosques, churches and bridges with complex geometric features [6, 34, 35, 39].

Thus, an analysis was carried out which presents the structural behavior of a historical bridge with high accuracy and reliability. It is thought that this proposed approach facilitates, accelerates the modelling steps, and in this sense brings innovation to the literature. In addition, no analytical studies on the assessment of the Sillyon bridge have been found in the literature.

2 Sillyon bridge

Ayvalıkemer (Sillyon) bridge is located within the borders of Yanköy Village, Serik District of Antalya Province in Turkey. It is located on Koducak stream, which passes about 1 km south west of Sillyon antique city. There is no inscription on the Sillyon Bridge indicating the date of construction or repair. No archive record was found about its history. Considering the architectural features of the bridge, large block stones used in its construction, round arches, its proximity to the ancient city of Sillyon, and similar bridges in its immediate environment, it can be dated to the Roman period, to the second century. It has a length of 37 m. It has a deck width of 4.7 m. It has three arches and the middle arch is larger than the other two. The floor covering and railing of the bridge has not survived to the present day. Due to the stone foundation being below the water level, material losses have been occurred on the stone surface depending on the streams and the alluviums carried. Color change and complete extinction were observed in some parts. In summary, the bridge elements (e.g., spandrel walls, two flood splitters, stone foundation and three arches) have partially survived by preserving its original qualities apart from partial material losses (Fig. 1a) [51]. In addition, the Western Mediterranean geography, which includes the ancient city

Fig. 1 Sillyon Bridge **a** before and **b** after restoration (downstream direction)

of Sillyon and its bridge, witnessed many earthquakes in history and the historical buildings were exposed to destructive damage [52–55]. As a result, it was restored in 2018 by the General Directorate of Highways in accordance with the original (Fig. 1b).

3 Material and methods

3.1 Methodology, terrestrial laser scanning technologies and data set

The Methodology carried out in this study is summarized in Fig. 2. There are two different methods to create the analysis model, preferably first, the "CAD based solid model" has been created, and then meshing this single solid by the macro modelling technique is prepared.

Digital photogrammetry and terrestrial laser scanning (TLS) method are among the best measurement methods for historical buildings due to their high spatial resolution capabilities. In particular, TLS method has replaced traditional measurement methods recently. It is one of the best examples of technological advances in terms of geomatic methods to measure the 3D geometry of objects without direct contact with objects [56]. It facilitates the modelling of sections (e.g., vaults, bridge legs) that are difficult to reach. With this method, millions of points are obtained with high precision and accuracy [57]. In the literature, there are many studies on the use of terrestrial laser scanners in historical construction and bridge measurements [11, 56–60].

In this study, FARO Focus^{3D} X130 laser scanner was used. Under normal light and reflection conditions, it has a sensitivity of 2 mm and can measure between 0.6 and 130 m. The scanner has the ability to rotate in the direction of 300° vertical axis and 360° horizontal axis. The weight of the scanner is 5.2 kg. It has a color resolution of 70 megapixels and can obtain 976,000-point data per second [61]. In this study, the distances between the measurement stations and the bridge are generally kept as low as possible within the range of 5–8 m and the angular resolution of the scanning process is determined as 0.08°. Point clouds contain many data other than bridge details. For this reason, unneeded points in the scanning data are removed before creating a 3D point cloud. After removing the data, the point clouds obtained from different stations were combined in a common coordinate system to obtain a single 3D point cloud of the entire bridge. High resolution orthophotos were prepared using the combined three-dimensional and color scanning data obtained. 3D models of historical buildings will be an important reference data for restoration works. If these historical buildings are damaged or destroyed due to any situation, they serve as archives in digital environment. In addition, when the point clouds created by TLS method are transformed into solid models, they also contribute to analysis on historical buildings.

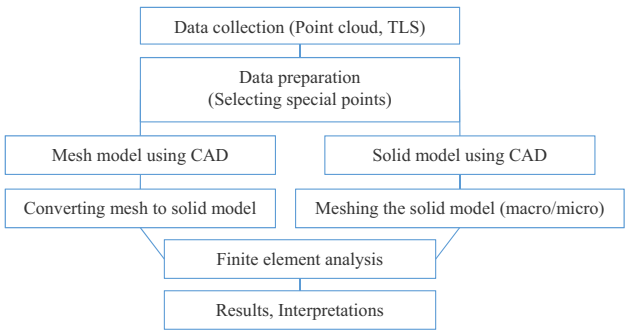

Fig. 2 Methodology of TLS based structural analysis

3.2 Macro modelling method

When modelling historical masonry structures, two basic assumptions are taken into account: macro modelling and micro modelling. In the micro modelling method, stone or brick, which is the carrier structural material, is modelled separately, and the mortar providing binding effect is modelled separately [62, 63]. This modelling is divided into two as detailed and simplified among themselves. In the macro modelling method, modelling is done by accepting the structural materials as a single material, not separate (Fig. 3a–c).

Macro modelling technique is preferred in the analysis of large structures, since a finite number of finite elements is required than the number of nodes and elements used in micro modelling techniques [65]. This approach is generally used in the modelling of walls, feet, buttresses, arches and vaults of complex system masonry structures. However, in this approach, no detailed information can be obtained about crack geometry, spread and collapse behavior. In this approach, the material is considered composite. Stone or brick and mortar are homogenized and transformed into a single material feature [66]. It is based on modelling the masonry structure with a homogeneous anisotropic environment without any discrimination and difference between stone, brick and mortar. At the same time, using the composite material theory, homogenization is performed by accepting that the masonry unit has a homogeneous and isotropic material feature [67]. Lourenço et al. [68] performed numerical modelling of masonry units with a homogenization method called "Unit cell method" (Fig. 3d).When a simple cell taken from the masonry wall is examined, it is used in the material parameters taking into account the participation rates of mortar and brick and can be considered as a single material. Lourenço [68] proposes Eq. (1) for the calculation of other material parameters, especially the elasticity module

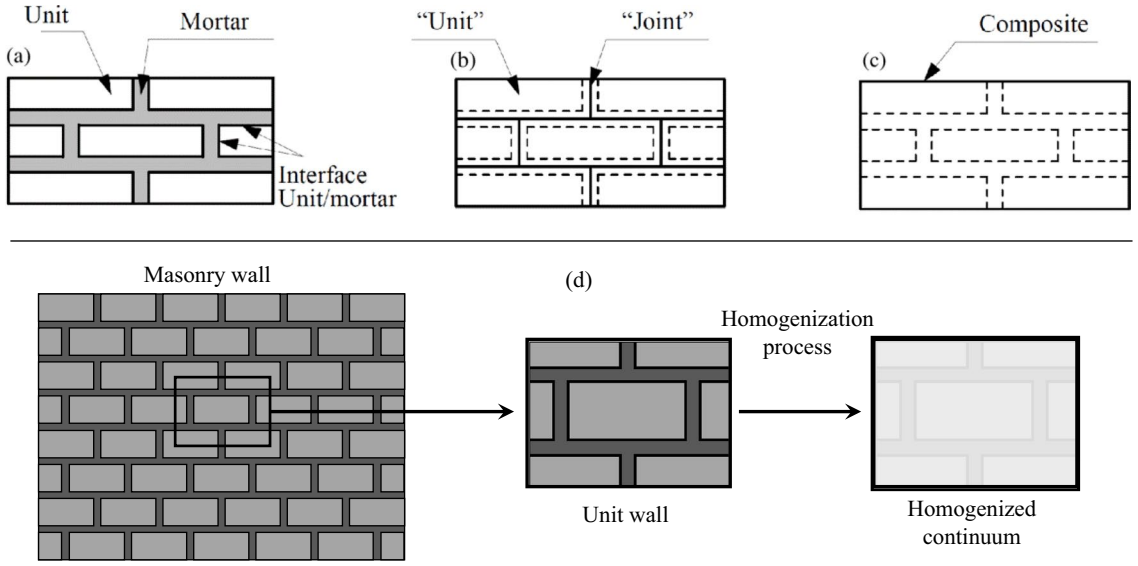

Fig. 3 Modelling techniques in masonry walls **a** detailed micro modelling **b** simplified micro modelling **c** macro modelling [64] **d** Homogenization by unit cell method

for brick and mortar. In this study, Eq. (1) is used to define the linear initial part of the behavior:

$$E_{wa} = \frac{t_s + t_m}{\frac{t_s}{E_s} + \frac{t_m}{E_m}} \delta_w \tag{1}$$

here; E_{wa} is the average modulus of elasticity for the composite material obtained, t_m is the mortar thickness, t_s is the brick thickness, E_m is the modulus of elasticity of the mortar, E_s is the modulus of elasticity of the brick. δ_w is a coefficient ranging from 0 to 1, which indicates the effectiveness of the bond between brick and mortar, and can be accepted as 0.5 for an average structure.

The Concrete Damage Plasticity (CDP) material model, which has been widely used in recent years for the stress–strain behavior of brittle materials, is also used in this study to express the nonlinear part of the behavior [69–71]. Compressive stress–strain behavior of the material and uniaxial tensile stress–strain behavior is defined by the relations [72, 73] shown in Eqs. (2,3):

$$\sigma_c = f_{co} \frac{n\left(\frac{\varepsilon_c}{\varepsilon_{co}}\right)}{(n-1) + \left(\frac{\varepsilon_c}{\varepsilon_{co}}\right)^n} \quad \varepsilon_{co} = 2.7 \times 10^{-4} \left(\sqrt[4]{f_{co}}\right) \quad n = 0.4 \times 10^{-3} f_{co} + 1 \text{ (MPa)} \tag{2}$$

$$\sigma_t = f_{to} \left(\frac{\varepsilon_{to}}{\varepsilon_t}\right)^{(0.4)} \quad \varepsilon_{to} = \frac{f_{to}}{E_c} \tag{3}$$

In Eq. (2), f_{co} and ε_{co} denotes compressive strength and strain at maximum stress. f_c and ε_c are compressive stresses and strains at any point on the stress–strain curve. The steepness of this curve is controlled by the empirical coefficient "n". σ_t and ε_t in Eq. (3) are the tensile stresses of material and the strains corresponding to these stresses, respectively. f_{to} is the tensile strength, ε_{to} is the unit strain corresponding to f_{to} and E_c is the elasticity modulus of the material.

There are several methods used to determine the material properties of masonry stonewalls. One of these methods is given in EUROCODE-6 [74]. Here, a common and equivalent material property can be determined by considering the geometrical and material properties of the different materials working together. The strength of the composite material consisting of natural stone and mortar in EUROCODE-6 is as given in Eq. (4):

$$f_{co} = K \times f_{stone}^{0.7} \times f_{mortar}^{0.3} \tag{4}$$

here; K value is determined according to EUROCODE 6—Table 3.3, for the dimensioned natural stone type and Group-1 ground class, 0.45 value is selected from the table.

The tensile strength of the masonry wall is mostly related to the strength of the mortar material, which has less value than the stone parts. For this reason, to define the upper limit of the tensile stress in the masonry wall, the minimum tensile strength of the mortar can be used as f_{to} value.

In the analysis of historical structures, four different methods can be used, such as static analysis under vertical and horizontal loads, free vibration analysis (modal analysis), behavior spectrum analysis and analysis in the time domain. Correct interpretation of the analyzes made is critical in the renovation or strengthening phase of the building. Strengthening and renewal required in the structure are applied depending on these interpretations.

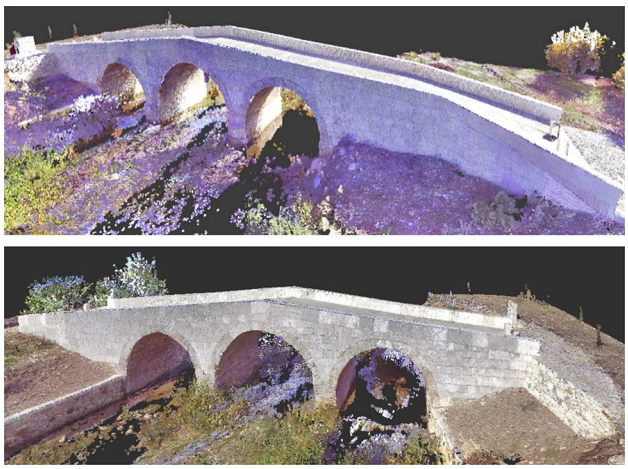

Fig.4 Point clouds obtained by terrestrial laser scanning (upstream and downstream direction)

4 Findings

4.1 CAD based solid model preparation using point cloud data and macro modelling

After the restoration works of the bridge were completed, the point cloud and orthophoto image were produced by the terrestrial laser scanning method. Point cloud file has been transferred to ReCap 2020 software [75] (Fig. 4). First, in the point cloud file, arches, handrails, foundations, folds and points deemed necessary from all surfaces were determined separately from the upstream and downstream sides to model the structure exactly. In AutoCAD 2020 software [76], a solid model was produced using some tools (e.g., 3DPoly, Surface, Loft, Patch, Sculpt) (Fig. 5).

Thus, the entire bridge as a single solid piece can be exported to the finite element analysis program. The finite element model and its mesh pattern of the bridge prepared using the macro modelling technique are shown in Fig. 6. In the modelling, it was assumed that the foundation on which the bridge is located is totally rigid.

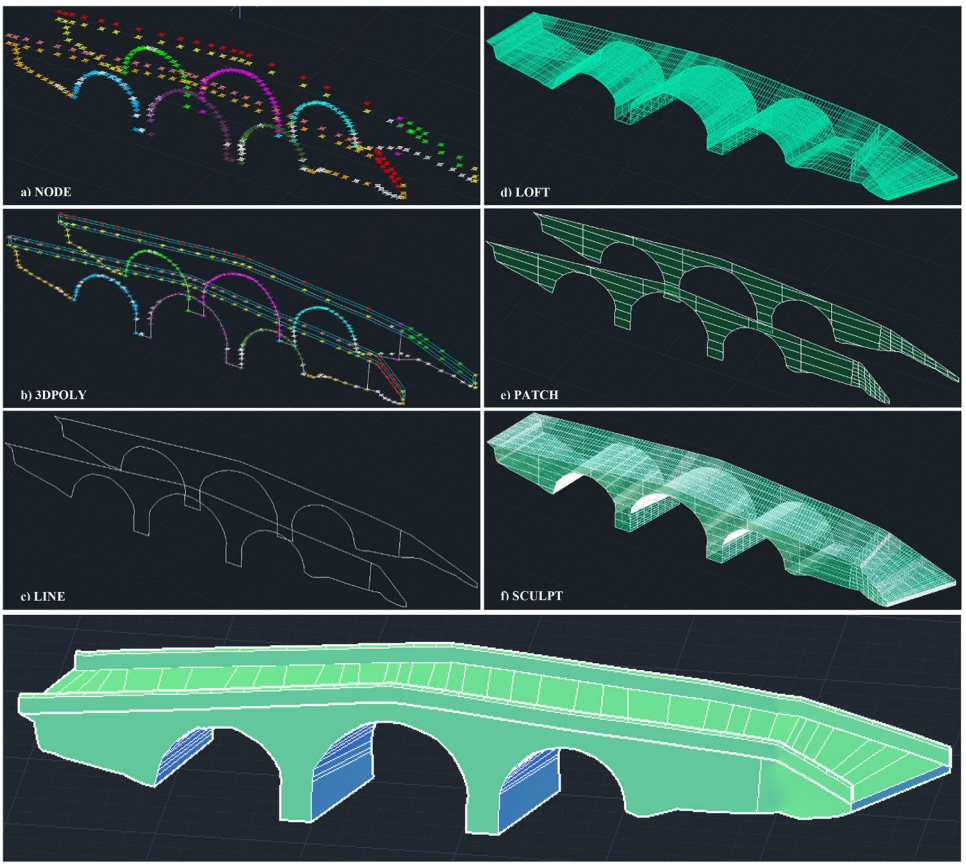

Fig. 5 Solid model production steps and perspective view of solid model in AutoCAD

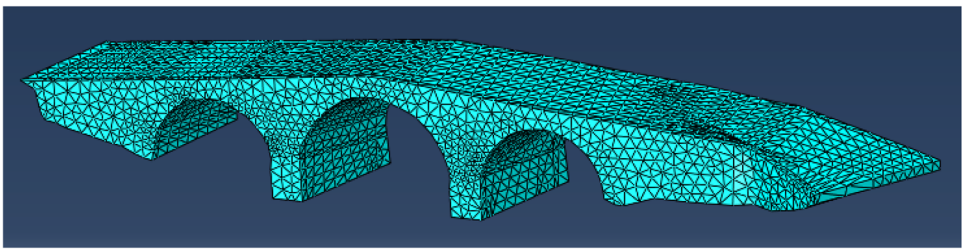

Fig. 6 Perspective view of the finite element model

4.2 Material and load types for macro modelling

In this study, Concrete Damaged Plasticity (CDP) material model was used to describe the inelastic behavior of homogenized structure [69, 70]. The tension meridians of the failure surface of the CDP, which is developed with the modification of the Drucker Prager model, are reduced with the K coefficient, and the linear meridians are transformed into parabola with the eccentricity (e) parameter. Dilation angle (β) is obtained from the angle between mises equivalent effective stress and the hydrostatic axis. f_{b0}/f_{c0} is the ratio of the biaxial compressive strength of the material to the uniaxial compressive strength. The CDP parameters considered for the whole structure are assumed as; β, 36; e, 0.1; f_{b0}/f_{c0}, 1.16 and K, 0.667 respectively [71].

During the restoration study, material tests were performed on the travertine stone that forms the historical bridge (Table 1). The "Denizli, Kocabağ" travertine, which is compatible with the original material properties, was decided to use in the restoration. In this study, the modulus of elasticity required for the linear part of the analysis is considered as the arithmetic mean of the vertical and horizontal test results. The Poisson ratio of travertine stone was taken into consideration as 0.3 in accordance with the article prepared by Çelik and Çobanoğlu [77].

"Master Emaco S285 TIX" repairing mortar was used as a binder between stones in restoration. Only one elasticity module is needed for the macro model of the composite bridge. To obtain this value, taking into account the common effect of the bonding material and stones, the expression of Lourenço given in Eq. (1) has been used. The average modulus of elasticity (E_{wa}) value obtained for the wholestone wall pattern with an average edge length of 300 mm and a joint spacing of 10 mm is shown in Table 1. The tensile strength (f_{to}) of the whole masonry structure was considered as 0.15 MPa, because of the mortar bond strength is weaker than the tensile strength of travertine stone. The material models and damage parameters considered to represent the compressive and tensile behavior of the homogenized material of the masonry bridge are shown in Fig. 7.

In the static analysis, besides self-weight (G) load, 150 kg/m^2 live load (Q) and 500 kg/m^2 flood load (W) acting from the upstream direction of the bridge were taken into account. If these loading conditions are converted to SI unit system, 0.001471 N/mm^2 as live load (Q) and 0.049033 N/mm^2 as flood load (W) are obtained. The parapet walls that

Table 1 Mechanical properties of materials

Material name	Properties	Value	Unit
Travertine stone	Density	22.60	kN/m^3
	Compressive strength in vertical direction (σ_{sv})	31.25	N/mm^2
	Compressive strength in horizontal direction (σ_{sh})	41.92	N/mm^2
	Average compressive strength (σ_{sa})	36.59	N/mm^2
	Tensile strength	2.81	N/mm^2
	Modulus of elasticity in vertical direction (E_{sv})	26,400	N/mm^2
	Modulus of elasticity in horizontal direction (E_{sh})	35,200	N/mm^2
	Average modulus of elasticity (E_{sa})	30,800	N/mm^2
Mortar	Density	20.30	kN/m^3
	Compressive strength (σ_{mc})	15	N/mm^2
	Bond strength (σ_{mt})	0.15	N/mm^2
	Modulus of elasticity (E_m)	16,000	N/mm^2
Whole masonry structure	Average stone dimension (t_s)	300	mm
	Average mortar thickness (t_m)	10	mm
	Calculated compressive strength (f_{co})	12.60	N/mm^2
	Considered tensile strength (f_{to})	0.15	N/mm^2
	Calculated modulus of elasticity (E_{wa})	14,954	N/mm^2

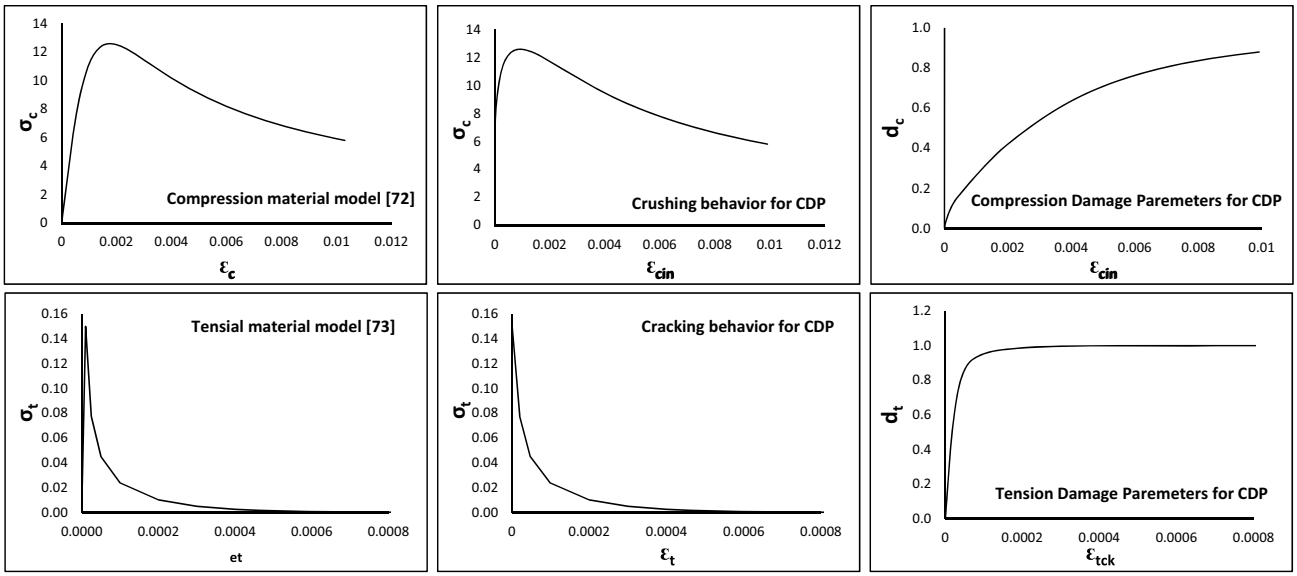

Fig. 7 Material models and damage parameters for CDP [72, 73]

do not contribute to bridge strength are considered only as distributed load in modelling (Fig. 8). The parapet load, which was calculated as 450 kg/m, was applied as a distributed load on the upstream and downstream sides.

4.3 Structural analysis using macro modelling

For the analysis, nonlinear explicit dynamic solution method was used. Explicit solution method was preferred in order not to encounter numerical instabilities and convergence problems caused by brittle damage and sudden stiffness losses seen in nonlinear models. In the model, homogenized stone and mortar structure represented with C3D8R (8-node brick elements with reduced integration) solid elements using macro modeling method.

Totally, eight analyzes were performed on the macro model of the historical bridge. These are; dead load analysis (*G*), live load analysis (*Q*), upstream direction flood load analysis (*W*), free vibration analysis (*S*) for the first fifty modes, horizontal *X* direction spectrum analysis (SPECX), horizontal *Y* direction spectrum analysis (SPECY), vertical *Z* direction spectrum analysis (SPECZ) and spectrum analysis (SPECXYZ) in all *XYZ* directions simultaneously. The loading combinations considered for these analyzes are given in Table 2.

4.3.1 Static analysis for vertical and horizontal loads

The static analysis of the Ayvalıkemer (Sillyon) bridge for vertical and horizontal loads is important in terms of obtaining the stress distribution under the dead and moving loads and determining the damage zones that may occur. This loading, which does not take into account horizontal loads such as earthquake and wind, is actually the usual loading condition of the building and is expected to be carried without any problem. In static analysis, the weight of the building as dead loads, and the loads that may occur during the transition over the structure as live loads are considered.

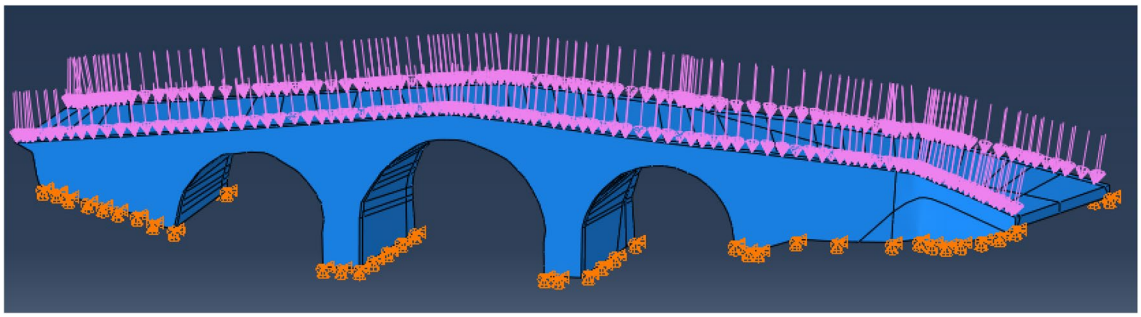

Fig. 8 Parapet load distribution in finite element model

Table 2 Load combinations considered in macro modelling

Analysis type	Analysis considered in the combination	Combination type
Static analysis	Dead load analysis	G
	Dead and live load analyzes	G + Q
	Dead and flood load analyzes	G + W
Response spectrum analysis	Dead and horizontal X direction spectrum analyzes	G + SPECX
	Dead and horizontal Y direction spectrum analyzes	G + SPECY
	Dead and vertical Z direction spectrum analyzes	G + SPECZ
	Dead and all XYZ directions spectrum analyzes	G + SPECXYZ

Because of these loads, the analysis results of the stress and displacement obtained are shown in the Fig. 9.

4.3.2 Free vibration analysis (modal analysis)

Modal analysis has been performed to determine the dynamic characterization of the Ayvalıkemer (Sillyon) bridge and to provide the sub-data needed by the response spectrum analysis. In this analysis; free vibration periods, mode shapes and mass participation rates of the building are determined. The contribution of each free vibration mode of the structure to the behavior of the building system is obtained separately. Response spectrum analysis is done by combining the contribution of each mode (mode superposition method) so that the dynamic behavior of the structure is determined [78].

In this study, the free vibration characteristics of the Ayvalıkemer (Sillyon) bridge structure have been tried to be determined analytically. A suitable number of mode shape vectors should be taken into account for the response spectrum analysis of the structure. For this purpose, it has been understood that it will be sufficient to determine the first 50 modes of the building according to the mass participation rates in the global directions. The free vibration characteristics of the structure are presented in Table 3 and the related 1–5th and 50th mode shape vectors are presented in Fig. 10.

4.3.3 Response spectrum analysis

Maximum value of parameters such as stress and displacement is required in the design of structural systems. Therefore, using the spectrum of the earthquake motion, the most unfavorable values are directly obtained without the need

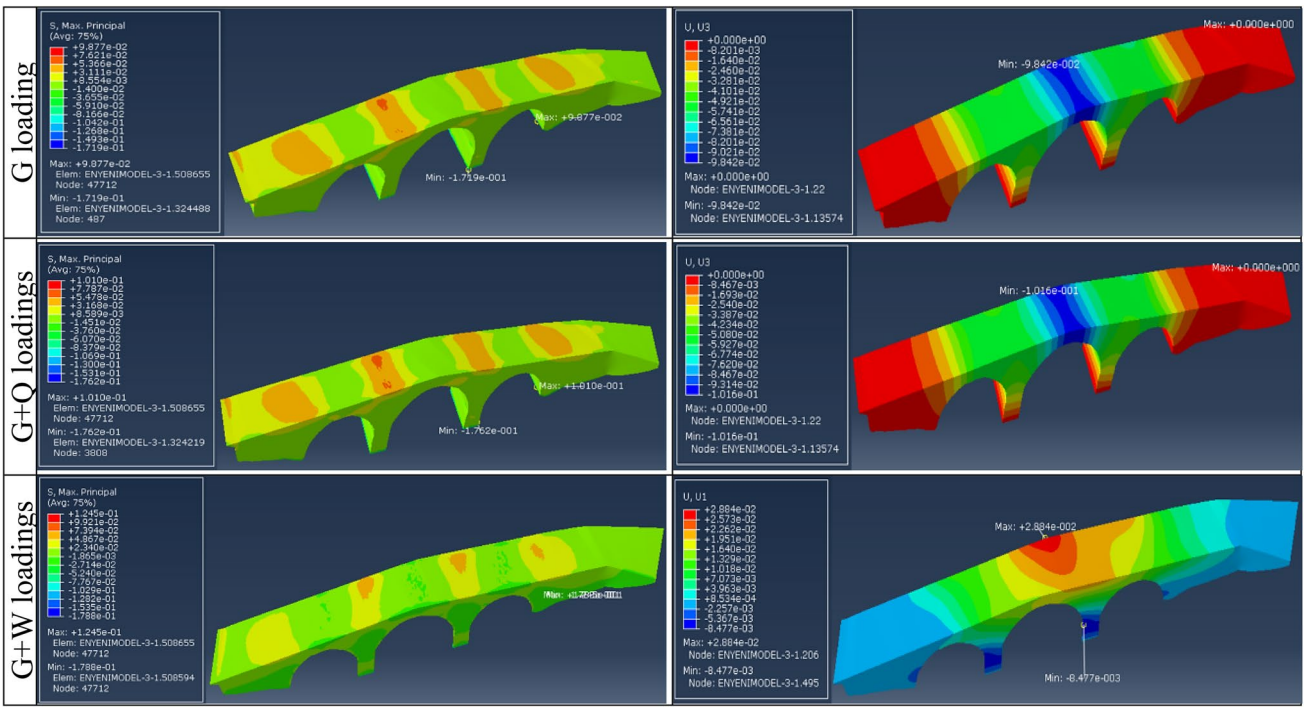

Fig. 9 Principal normal stresses and vertical displacements under static loads

Table 3 Modal periods and frequencies of the structure (mode 1–50)

Mode number	Frequency (1/sn)	Period (sn)
1	27.937	0.035795
2	44.829	0.022307
3	45.844	0.021813
4	54.448	0.018366
5	63.246	0.015811
10	86.525	0.011557
15	116.59	0.008577
20	139.18	0.007185
25	159.60	0.006266
30	187.35	0.005338
35	197.82	0.005055
40	212.00	0.004717
45	227.61	0.004393
50	239.00	0.004184

for numerical analysis that is long and complex. Since the spectral curves give only the greatest values and are not sufficient in determining the contributions of various modes for a given moment, some mathematical approaches have been developed for the calculation. One of these approaches is the Complete Quadratic Combination (CQC) method.

Response spectrum analysis was performed in global directions with macromodelling of the Ayvalıkemer (Sillyon) bridge structure. For this purpose, bridge coordinates were treated to interactive Web App (AFAD Turkey Earthquake Hazard Maps) to determine the seismicity of the bridge area. With the data obtained here, the formulas in Turkish Building Earthquake Code 2018 [79] were used to create the earthquake spectrum curves. The resulting horizontal and vertical elastic design spectrum curves are shown in Fig. 11. To be used in obtaining curves; damping ratio, 0.05; local ground class, ZE; short period map spectral acceleration coefficient (S_s), 0.519; map spectral acceleration coefficient for 1.0 s period (S_1), 0.138; short period design spectral acceleration coefficient (S_{DS}), 0.8665; the design spectral acceleration coefficient for 1.0 s period (S_{D1}), 0.53240, was taken into account.

In the response spectrum analysis, four different load combinations were considered shown as in Table 2. With these combinations, the maximum stress and displacement values that can occur in the structure as a result of the loading acting separately in the global *X, Y, Z* directions and simultaneously in these three directions were obtained (Fig. 12).

5 Conclusions

Origin of the stone used in Ayvalıkemer (Sillyon) historical bridge is travertine stone. A preliminary investigation was carried out on which quarry would be extracted from the nearby area, and it was determined that the stone could be obtained from the Kocabaş quarry of Denizli in Turkey. After the supply of the material to be used, the renovation project was prepared and the works were completed by preserving the original structure. At the end of the restoration work, the final version of the bridge was scanned and archived by the TLS (Terrestrial Laser Scanning) method.

In this study, it has been understood that the point cloud obtained as a result of terrestrial laser scanning technique

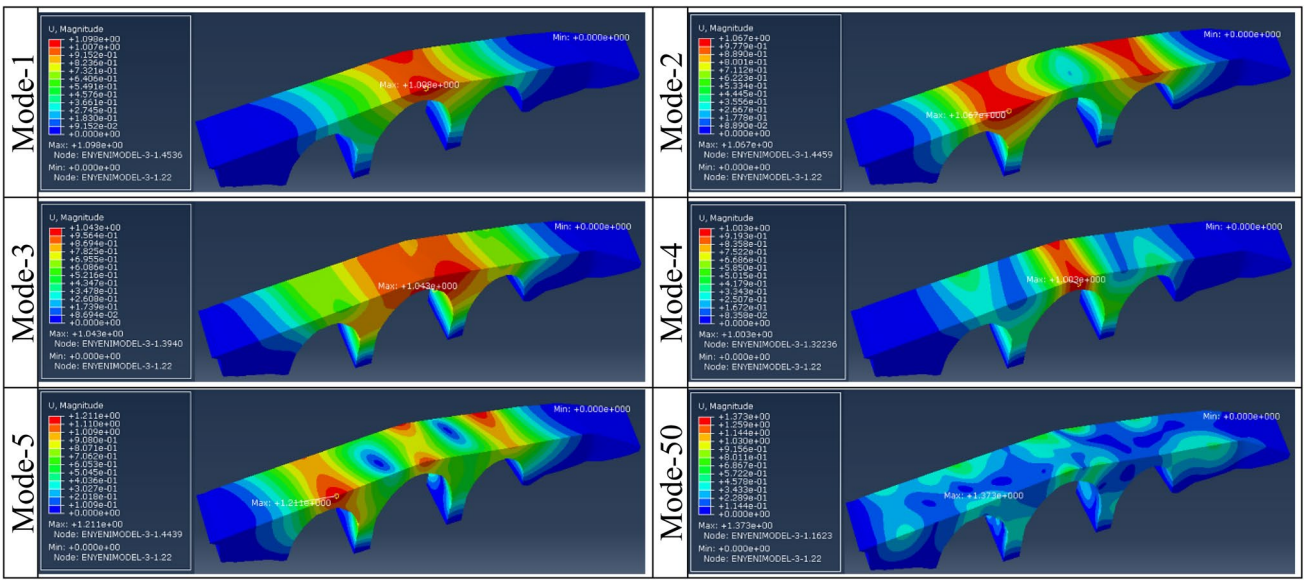

Fig. 10 Mode shape vectors of various modes

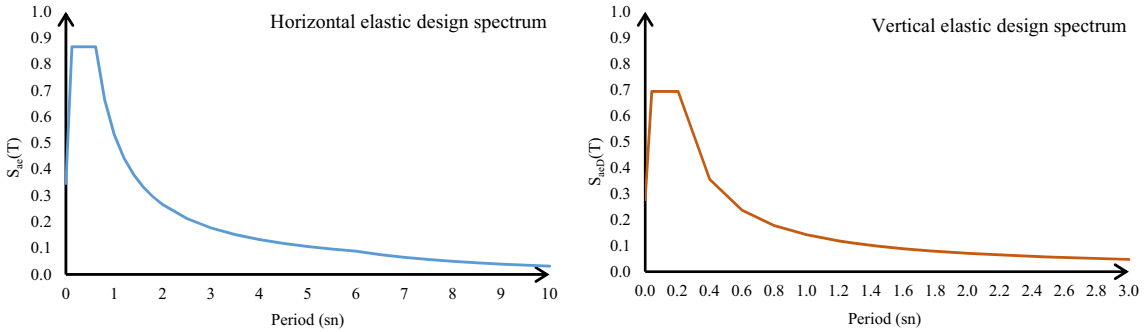

Fig. 11 Horizontal and vertical elastic design spectrum curves for the region

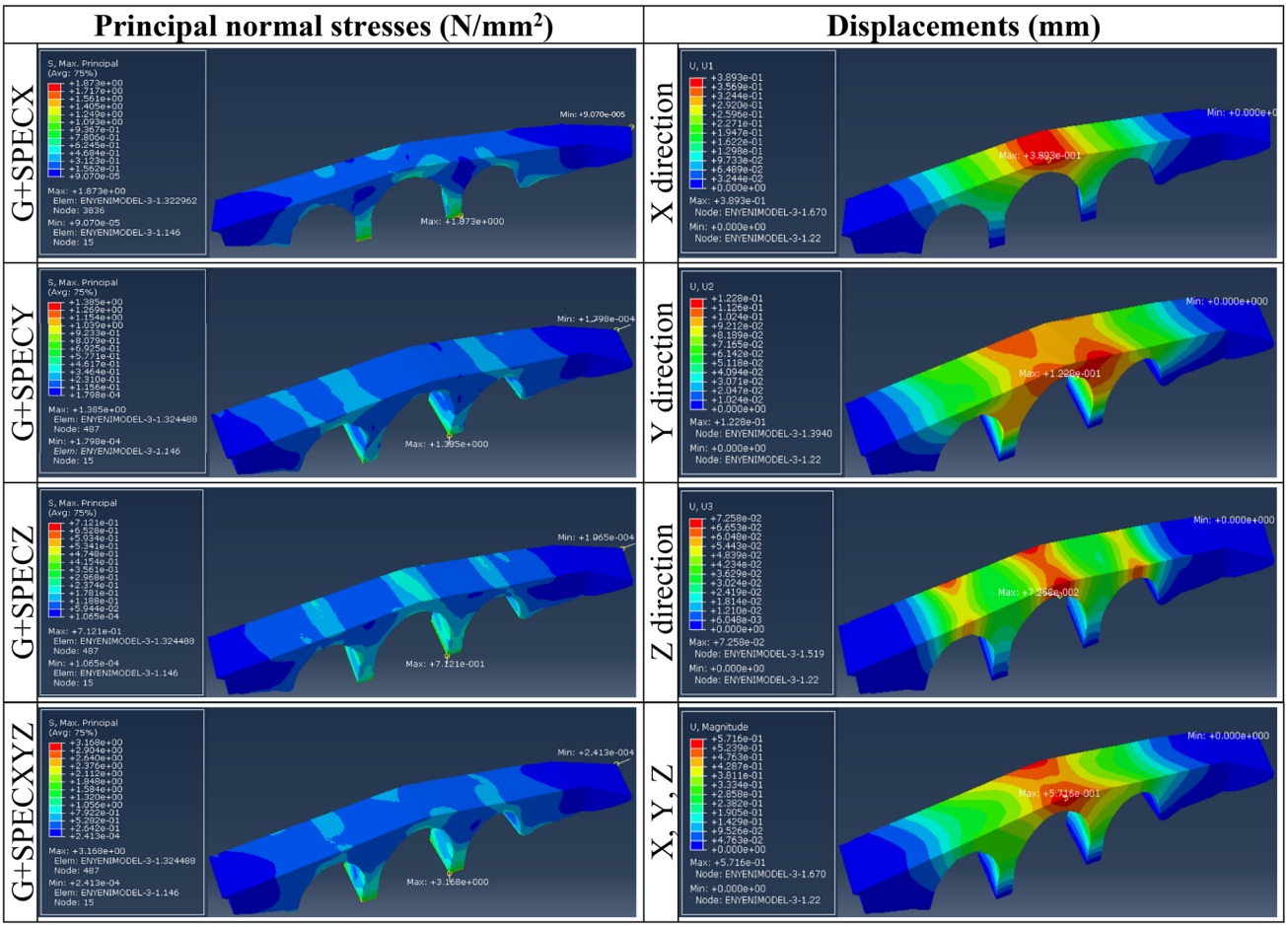

Fig. 12 Principal normal stress and displacement values for various load combinations

provides a very fast and highly accurate data for determining the structural geometry that will support the structural analysis. A computer-aided solid element model of the building was created using the point cloud data. Following the completion of the modelling, load and material assumptions were made and static and dynamic analyzes of the structure were carried out, respectively.

The analysis of restored Ayvalıkemer (Sillyon) historical bridge was performed by using macro modelling technique. Analytical study was carried out on a solid model of the structure. It has been seen that the principal normal stress and displacement values determined in the analyzes remained in the initial elastic part of the material defined for the whole masonry structure (Figs. 7, 9, 10, 11, 12,

Table 1). Therefore, despite the preparation of a numerical model including the inelastic material behavior by the CDP, no damage result in the form of crushing or cracking was obtained under the considered loadings at the components of the historical bridge. The greatest compressive stress was calculated as 3.168 MPa as a result of G + SPECXYZ response spectrum analysis performed for all global directions (Fig. 11). It has been determined that this stress does not exceed the compressive strength of both mortar and travertine stone and can safely carry the loads on the bridge, which is closed to vehicle traffic. It has been observed that the point cloud obtained by TLS method is very useful for modelling and analytical studies that will be carried out for historical buildings.

Acknowledgements The authors gratefully acknowledge the following collaborators with Akdeniz University: Architect İbrahim CEYLAN and General Directorate of Highways in Turkey for the support in the laser scanner survey of the Ayvalıkemer (Sillyon) Bridge.

Author contributions OSB, ET, and EE designed the research, performed the study, and wrote the paper.

Funding No funding information available.

Data availability The datasets used during the current study is available from the corresponding author on reasonable request.

Code availability The macro model analyzed during the current study is available from the corresponding author on reasonable request.

Declarations

Conflicts of interest The authors declare that they have no conflict of interest.

References

1. Leonov AV, Anikushkin MN, Ivanov AV, Ovcharov SV, Bobkov AE, Baturin YM (2015) Laser scanning and 3D modelling of the Shukhov hyperboloid tower in Moscow. J Cult Herit 16(4):551–559. https://doi.org/10.1016/j.culher.2014.09.014
2. Costa-Jover A, Ginovart JL, Coll-Pla S, Piquer ML (2019) Using the terrestrial laser scanner and simple methodologies for geometrically assessing complex masonry vaults. J Cult Herit 36:247–254. https://doi.org/10.1016/j.culher.2018.10.003
3. Pachón P, Castro R, García-Macías E, Compan V, Puertas E (2018) E. Torroja's bridge: tailored experimental setup for SHM of a historical bridge with a reduced number of sensors. Eng Struct 162:11–21. https://doi.org/10.1016/j.engstruct.2018.02.035
4. Altunisik AC, Kalkan E, Okur FY, Ozgan K, Karahasan OS, Bostanci A (2019) Non-destructive modal parameter identification of historical timber bridges using ambient vibration tests after restoration. Measurement 146:411–424. https://doi.org/10.1016/j.measurement.2019.06.051
5. Kushwaha SKP, Raghavendra S, Pande H, Agrawal S (2020) Analysis and integration of surface and subsurface information of different bridges. J Indian Soc Remote Sens 48(2):315–331. https://doi.org/10.1007/s12524-019-01087-2
6. Hacıefendioğlu K, Başağa HB, Banerjee S (2017) Probabilistic analysis of historic masonry bridges to random ground motion by Monte Carlo Simulation using Response Surface Method. Constr Build Mater 134:199–209. https://doi.org/10.1016/j.conbuildmat.2016.12.101
7. Simos N, Manos GC, Kozikopoulos E (2018) Near-and far-field earthquake damage study of the Konitsa stone arch bridge. Eng Struct 177:256–267. https://doi.org/10.1016/j.engstruct.2018.09.072
8. Ferrari R, Cocchetti G, Rizzi E (2016) Limit Analysis of a historical iron arch bridge. Formulation and computational implementation. Comput Struct 175:184–196. https://doi.org/10.1016/j.compstruc.2016.05.007
9. Toker S, Ünay Aİ (2004) Mathematical modelling and finite element analysis of masonry arch bridges. Gazi Univ J Sci 17(2):129–139
10. Sánchez-Aparicio LJ, Bautista-De Castro Á, Conde B, Carrasco P, Ramos LF (2019) Non-destructive means and methods for structural diagnosis of masonry arch bridges. Autom Constr 104:360–382. https://doi.org/10.1016/j.autcon.2019.04.021
11. Riveiro B, De Jong MJ, Conde B (2016) Automated processing of large point clouds for structural health monitoring of masonry arch bridges. Autom Constr 72:258–268. https://doi.org/10.1016/j.autcon.2016.02.009
12. Conde B, Drosopoulos GA, Stavroulakis GE, Riveiro B, Stavroulaki ME (2016) Inverse analysis of masonry arch bridges for damaged condition investigation: application on Kakodiki bridge. Eng Struct 127:388–401. https://doi.org/10.1016/j.engstruct.2016.08.060
13. Stavroulaki ME, Riveiro B, Drosopoulos GA, Solla M, Koutsianitis P, Stavroulakis GE (2016) Modelling and strength evaluation of masonry bridges using terrestrial photogrammetry and finite elements. Adv Eng Softw 101:136–148. https://doi.org/10.1016/j.advengsoft.2015.12.007
14. Yavuz UC (2012) Tarihi Yapılarda Statik Güçlendirme Teknikleri. Expertise Thesis. Ministry of Culture and Tourism, General Directorate of Cultural Heritage and Museums. Ankara, Turkey, pp 71 (**in Turkish**)
15. Jaafar HA, Meng X, Sowter A, Bryan P (2017) New approach for monitoring historic and heritage buildings: using terrestrial laser scanning and generalised procrustes analysis. Struct Control Health Monit 24(11):e1987. https://doi.org/10.1002/stc.1987
16. Sánchez-Rodríguez A, Riveiro B, Conde B, Soilán M (2018) Detection of structural faults in piers of masonry arch bridges through automated processing of laser scanning data. Struct Control Health Monit 25(3):e2126. https://doi.org/10.1002/stc.2126
17. Law DW, Silcock D, Holden L (2018) Terrestrial laser scanner assessment of deteriorating concrete structures. Struct Control Health Monit 25(5):e2156. https://doi.org/10.1002/stc.2156
18. Yorulmaz M (1984) Building construction under seismic conditions in the Balkan region, 3rd edn. United Nations Industrial Development Organization. Executing agency for the United Nations Development Programme, pp 151
19. Fanning PJ, Boothby TE (2001) Three-dimensional modelling and full-scale testing of stone arch bridges. Comput Struct 79(29–30):2645–2662. https://doi.org/10.1016/S0045-7949(01)00109-2
20. Brencich A, Sabia D (2008) Experimental identification of a multi-span masonry bridge: the Tanaro Bridge. Constr Build

Mater 22(10):2087–2099. https://doi.org/10.1016/j.conbuildmat.2007.07.031
21. Sevim B, Bayraktar A, Altunişik AC, Atamtürktür S, Birinci F (2011) Finite element model calibration effects on the earthquake response of masonry arch bridges. Finite Elem Anal Des 47(7):621–634. https://doi.org/10.1016/j.finel.2010.12.011
22. Milani G, Lourenço PB (2012) 3D non-linear behavior of masonry arch bridges. Comput Struct 110:133–150. https://doi.org/10.1016/j.compstruc.2012.07.008
23. Castellazzi G, Miranda SD, Mazzotti C (2012) Finite element modelling tuned on experimental testing for the structural health assessment of an ancient masonry arch bridge. Math Problems Eng. https://doi.org/10.1155/2012/495019
24. Guarnieri A, Milan N, Vettore A (2013) Monitoring of complex structure for structural control using terrestrial laser scanning (TLS) and photogrammetry. Int J Arch Heritage 7(1):54–67. https://doi.org/10.1080/15583058.2011.606595
25. Pelà L, Aprile A, Benedetti A (2013) Comparison of seismic assessment procedures for masonry arch bridges. Constr Build Mater 38:381–394. https://doi.org/10.1016/j.conbuildmat.2012.08.046
26. Korkmaz KA, Zabin P, Çarhoğlu AI, Nuhoğlu A (2013) Taş Kemer Köprülerin Deprem Davranışlarının Değerlendirilmesi: Timisvat Köprüsü Örneği. J Adv Technol Sci 2(1):66–75 (**in Turkish**)
27. Rafiee A, Vinches M (2013) Mechanical behaviour of a stone masonry bridge assessed using an implicit discrete element method. Eng Struct 48:739–749. https://doi.org/10.1016/j.engstruct.2012.11.035
28. Altunışık AC, Kanbur B, Genc AF (2015) The effect of arch geometry on the structural behavior of masonry bridges. Smart Struct Syst 16(6):1069–1089. http://doi.org/10.12989/sss.2015.16.6.1069
29. Karaton M, Aksoy HS, Sayın E, Calayır Y (2017) Nonlinear seismic performance of a 12th century historical masonry bridge under different earthquake levels. Eng Fail Anal 79:408–421. https://doi.org/10.1016/j.engfailanal.2017.05.017
30. Cakir F (2018) Structural performance assessment of historical Dilovası Sultan Süleyman (Diliskelesi) bridge in Turkey. Int J Electron Mech Mechatron Eng 8(3):1579–1588
31. Drygala I, Dulinska J, Bednarz Ł, Jasienko J (2018) Numerical evaluation of seismic-induced damages in masonry elements of historical arch viaduct. MS&E 364(1):012006
32. ABAQUS Tutorials (2019) Online Documentation Dassault Systemes Simulia User Assistance. Dassault Systemes, United States
33. Jahangiri V, Yazdani M, Marefat MS (2018) Intensity measures for the seismic response assessment of plain concrete arch bridges. Bull Earthq Eng 16(9):4225–4248. https://doi.org/10.1007/s10518-018-0334-8
34. Bautista-De Castro A, Sánchez-Aparicio LJ, Ramos LF, Sena-Cruz J, González-Aguilera D (2018) Integrating geomatic approaches, Operational Modal Analysis, advanced numerical and updating methods to evaluate the current safety conditions of the historical Bôco Bridge. Constr Build Mater 158:961–984. https://doi.org/10.1016/j.conbuildmat.2017.10.084
35. Caddemi S, Caliò I, Cannizzaro F, D'Urso D, Pantò B, Rapicavoli D (March 27–29, 2019) 3D Discrete macro-modelling approach for masonry arch bridges. The International Association for Bridge and Structural Engineering (IABSE) Symposium 2019. Guimarães, Portugal
36. Di Sarno L, da Porto F, Guerrini G, Calvi PM, Camata G, Prota A (2019) Seismic performance of bridges during the 2016 Central Italy earthquakes. Bull Earthq Eng 17(10):5729–5761. https://doi.org/10.1007/s10518-018-0419-4
37. Dall'Asta A, Leoni G, Meschini A, Petrucci E, Zona A (2019) Integrated approach for seismic vulnerability analysis of historic massive defensive structures. J Cult Herit 35:86–98. https://doi.org/10.1016/j.culher.2018.07.004
38. Hokelekli E, Yilmaz BN (2019) Effect of cohesive contact of backfill with arch and spandrel walls of a historical masonry arch bridge on seismic response. Periodica Polytech Civ Eng 63(3):926–937. https://doi.org/10.3311/PPci.14198
39. Zhao C, Xiong Y, Zhong X, Shi Z, Yang S (2020) A two-phase modeling strategy for analyzing the failure process of masonry arches. Eng Struct 212:110525. https://doi.org/10.1016/j.engstruct.2020.110525
40. Kujawa M, Lubowiecka I, Szymczak C (2020) Finite element modelling of a historic church structure in the context of a masonry damage analysis. Eng Failure Anal 107:104233. https://doi.org/10.1016/j.engfailanal.2019.104233
41. Banerji P, Chikermane S (2012) Condition assessment of a heritage arch bridge using a novel model updation technique. J Civ Struct Heal Monit 2:1–16. https://doi.org/10.1007/s13349-011-0013-9
42. Boscato G, Cin AD (2017) Experimental and numerical evaluation of structural dynamic behavior of Rialto Bridge in Venice. J Civ Struct Heal Monit 7:557–572. https://doi.org/10.1007/s13349-017-0242-7
43. Crotti G, Cigada A (2019) Scour at river bridge piers: real-time vulnerability assessment through the continuous monitoring of a bridge over the river Po, Italy. J Civ Struct Heal Monit 9:513–528. https://doi.org/10.1007/s13349-019-00348-5
44. Lorenzoni F, De Conto N, da Porto F, Modena C (2019) Ambient and free-vibration tests to improve the quantification and estimation of modal parameters in existing bridges. J Civ Struct Heal Monit 9:617–637. https://doi.org/10.1007/s13349-019-00357-4
45. Alexakis H, Lau FDH, De Jong MJ (2021) Fibre optic sensing of ageing railway infrastructure enhanced with statistical shape analysis. J Civ Struct Heal Monit 11:49–67. https://doi.org/10.1007/s13349-020-00437-w
46. Karimpour A, Rahmatalla S, Markfort C (2020) Identification of damage parameters during flood events applicable to multi-span bridges. J Civ Struct Heal Monit 10:973–985. https://doi.org/10.1007/s13349-020-00429-w
47. Potenza F, Rinaldi C, Ottaviano E, Gattulli V (2020) A robotics and computer-aided procedure for defect evaluation in bridge inspection. J Civ Struct Heal Monit 10:471–484. https://doi.org/10.1007/s13349-020-00395-3
48. Pieraccini M et al (2014) Dynamic identification of historic masonry towers through an expeditious and no-contact approach: Application to the "Torre del Mangia" in Siena (Italy). J Cult Herit 15(3):275–282. https://doi.org/10.1016/j.culher.2013.07.006
49. Castellazzi G et al (2015) From laser scanning to finite element analysis of complex buildings by using a semi-automatic procedure. Sensors 15:18360–18380. https://doi.org/10.3390/s150818360
50. Korumaz M et al (2017) An integrated terrestrial laser scanner (TLS), deviation analysis (DA) and finite element (FE) approach for health assessment of historical structures, a minaret case study. Eng Struct 153:224–238. https://doi.org/10.1016/j.engstruct.2017.10.026
51. GDH (2016) Antalya province, Serik district, Ayvalıkemer (Sillyon) bridge technical report. General Directorate of Highways, 13th Region, Antalya, Turkey, pp 19 (**in Turkish**)
52. Guidoboni E, Comastri A, Traina G (1994) Catalogue of Ancient Earthquakes in the Mediterranean Area up to the 10th Century. Roma Istituto Nazionale di Geofisica, Italy, pp 504

53. Bayburtluoğlu C (2003) Yüksek Kayalığın Yanındaki Yer-Arykanda. İstanbul, Homer Kitabevi, p 204 (**in Turkish**)
54. Duggan TMP (2004) A short account of recorded Calamities (earthquakes and plagues) in Antalya province and adjacent and related areas over the past 2300 years an incomplete list, comments and observations. Adalya 7:123–170
55. Softa M, Turan M, Sözbilir H (2018) Jeolojik, Arkeolojik ve Arkeosismolojik Veriler Işığında Myra Antik Kenti'nde Tarihsel Depremlere Ait Deformasyon Verileri, GB Anadolu. Geol Bull Turkey 61(1):51–73 (**in Turkish**). https://doi.org/10.25288/tjb.358177
56. Armesto J, Roca-Pardiñas J, Lorenzo H, Arias P (2010) Modelling masonry arches shape using terrestrial laser scanning data and nonparametric methods. Eng Struct 32(2):607–615. https://doi.org/10.1016/j.engstruct.2009.11.007
57. Lubowiecka I, Armesto J, Arias P, Lorenzo H (2009) Historic bridge modelling using laser scanning, ground penetrating radar and finite element methods in the context of structural dynamics. Eng Struct 31(11):2667–2676. https://doi.org/10.1016/j.engstruct.2009.06.018
58. Lubowiecka I, Arias P, Riveiro B, Solla M (2011) Multidisciplinary approach to the assessment of historic structures based on the case of a masonry bridge in Galicia (Spain). Comput Struct 89(17–18):1615–1627. https://doi.org/10.1016/j.compstruc.2011.04.016
59. Morer P, Arteaga ID, Armesto J, Arias P (2011) Comparative structural analyses of masonry bridges: an application to the Cernadela Bridge. J Cult Herit 12(3):300–309. https://doi.org/10.1016/j.culher.2011.01.006
60. Riveiro B, Morer P, Arias P, Arteaga ID (2011) Terrestrial laser scanning and limit analysis of masonry arch bridges. Constr Build Mater 25(4):1726–1735. https://doi.org/10.1016/j.conbuildmat.2010.11.094
61. Faro (2017) https://www.faro.com/news/faro-launches-new-x-series-laser-scanner-the-focus3d-x-130/ (Accessed 03 May 2020)
62. Adam JM, Brencich A, Hughes TG, Jefferson T (2010) Micro-modelling of eccentrically loaded brickwork: study of masonry wallettes. Eng Struct 32(5):1244–1251. https://doi.org/10.1016/j.engstruct.2009.12.050
63. Milani G, Lourenco PB, Tralli A (2006) Homogenization approach for the limit analysis of out-of-plane loaded masonry walls. J Struct Eng ASCE 132(10):1650–1663. https://doi.org/10.1061/(ASCE)0733-9445(2006)132:10(1650)
64. Lourenço PB (1996) Computational strategies for masonry structures. PhD thesis. Delft University of Technology, Netherlands, pp 220
65. Proske D, Gelder P (2009) Safety of historical arch bridges. Springer-Verlag, Heidelberg Dordrecht, London, p 366
66. Roca P, González JL, Oñate E, Lourenço PB (1998) Experimental and numerical issues in the modelling of the mechanical behavior of masonry. Structural analysis of historical constructions. II. CIMNE, Barcelona, pp 57–91
67. Proske D, Van Gelder P (2009) Safety of historical stone arch bridges. Springer Science and Business Media, pp 215
68. Lourenço PB, Vasconcelos G, Ramos L (2001) Assessment of the stability conditions of a Cistercian cloister. 2nd International Congress on Studies in Ancient Structures. İstanbul
69. Lubliner J, Oliver J, Oller S, Oñate E (1989) A plastic-damage model for concrete. Int J Solids Struct 25(3):299–326. https://doi.org/10.1016/0020-7683(89)90050-4
70. Lee JH, Fenves GL (1998) Plastic-damage model for cyclic loading of concrete structures. J Eng Mech (ASCE) 124:892–900. https://doi.org/10.1061/(ASCE)0733-9399(1998)124:8(892)
71. Bertolesi E, Milani G, Lopane FD, Acito M (2017) Augustus Bridge in Narni (Italy): seismic vulnerability assessment of the still standing part, possible causes of collapse, and importance of the roman concrete infill in the seismic-resistant behavior. Int J Arch Heritage Conserv Anal Restoration 11(5):717–746. https://doi.org/10.1080/15583058.2017.1300712
72. Popovics S (1973) A numerical approach to the complete stress-strain curve of concrete. Cem Concr Res 3(5):583–599. https://doi.org/10.1016/0008-8846(73)90096-3
73. Wang T, Hsu TTC (2001) Nonlinear finite element analysis of concrete structures using new constitutive models. Comput Struct 79(32):2781–2791. https://doi.org/10.1016/S0045-7949(01)00157-2
74. EN 1996-1-1:2005, EUROCODE 6 (2005) Design of masonry structures, Part 1–1: General rules for reinforced and unreinforced masonry structures. British Standards Institution. pp 123
75. ReCap (2020) 3D scanning software. Autodesk Inc, California
76. AutoCAD (2020) 3D computer-aided design software. Autodesk Inc, California
77. Çelik SB, Çobanoğlu İ (2019) Denizli travertenlerinde P ve S dalga hızları ile bazı fiziksel ve tek eksenli sıkışma dayanımı özellikleri arasındaki ilişkilerin araştırılması. Politeknik Dergisi 22(2):341–349 (**in Turkish**). https://doi.org/10.2339/politeknik.444370
78. Chopra AK (2019) Dynamics of structures: theory and applications to earthquake engineering, 5th edn. Pearson Education Limited, Harlow, p 992
79. TBEC (Turkish Building Earthquake Code) (2018) Specifications for buildings to be built in seismic areas. Ministry of Public Works and Settlement, Ankara